Eur. Phys. J. C 2, 181–195 (1998)

THE EUROPEAN PHYSICAL JOURNAL C

Elastic πN scattering to $\mathcal{O}(p^3)$ in heavy baryon chiral perturbation theory*

Martin Mojžiš

Department of Theoretical Physics, Comenius University, Mlynska dolina, SK-84215 Bratislava, Slovakia (e-mail: mojzis@fmph.uniba.sk)

Received: 29 April 1997

Abstract. The elastic πN scattering amplitude in the isospin limit is calculated in the framework of heavy baryon chiral perturbation theory, up to the third order. Threshold parameters like scattering lengths, volumes, effective ranges, etc. are compared with data. All relevant low energy constants are fixed from the available pion-nucleon data. A clear improvement in the description of data is observed, when going from the first two orders in the chiral expansion to the third one. The importance of even higher orders is suggested by the results.

1 Introduction

Constraints of chiral symmetry on pion-nucleon interactions were investigated in the sixties in terms of current algebra, and the prediction of the S-wave πN scattering lengths [1] was one of the most important results within this approach. In the eighties, the systematic method – called chiral perturbation theory (CHPT) – of calculating corrections to the current algebra results was invented [2], and it was applied to πN scattering up to order $\mathcal{O}(p^3)$ [3].

However, CHPT with nucleons is not as systematic as CHPT for light mesons, since the nucleon mass spoils one of the main virtues of CHPT – one-to-one correspondence between loop expansion and expansion in external momenta. This correspondence is valid for massless particles [4], so it works for the Goldstone bosons of the spontaneously broken chiral symmetry of QCD (pions, kaons and η), which are massless in the chiral limit of massless u, d and s quarks. Nonzero masses of light quarks, leading to nonzero masses of Goldstone bosons, are treated as a perturbation. The simultaneous expansion in external momenta and light quark masses is called chiral expansion. Nucleons, on the other hand, are massive even in the chiral limit and their masses cannot be treated as small perturbations. As a consequence, there is no more direct correspondence between loop and chiral expansions, and diagrams with arbitrary number of loops can contribute to a given chiral order.

This drawback was eliminated in the clever reformulation of CHPT with baryons [5] – called heavy baryon chiral perturbation theory (HBCHPT) – which, so to say, shifts the nucleon mass from the propagator to vertices of an effective Lagrangian and thus restores the loop–chiral correspondence. HBCHPT was applied to different processes up to order $\mathcal{O}(p^3)$ [6] (and even $\mathcal{O}(p^4)$ [7][8]), among others to the forward threshold πN scattering, from where the corrections to the S-wave πN scattering lengths up to order $\mathcal{O}(p^3)$ were calculated [9]. Recently also higher πN partial waves were calculated up to this order [10].

In these works, some of the low energy constants (LECs) of the $\mathcal{O}(p^3)$ πN Lagrangian were not determined from the fit to the πN data, instead they were estimated from the principle of resonance saturation, which had been shown to work very well in the mesonic sector [11], but in the baryonic sector it is just a working hypothesis.

The purpose of this paper is to calculate the full πN scattering amplitude in the isospin limit in HBCHPT to order $\mathcal{O}(p^3)$ and to fix the LECs contributing to this amplitude from the available experimental information. The paper is organized as follows. In Sect. 2 we summarize the previous results, needed for the calculation of the amplitude, in Sect. 3 the amplitude is calculated and in Sect. 4 it is confronted with data. Conclusions are summarized in Sect. 5, and some technical points and/or lengthy formulae are left to appendices.

2 HBCHPT of the pion-nucleon system

2.1 Effective Lagrangian

Our calculation of the elastic πN scattering is based on the low-energy expansion of the πN Lagrangian in HBCHPT

$$\mathcal{L}_{\pi\pi} + \widehat{\mathcal{L}}_{\pi N} = \mathcal{L}^{(2)}_{\pi\pi} + \mathcal{L}^{(4)}_{\pi\pi} + \ldots + \widehat{\mathcal{L}}^{(1)}_{\pi N} + \widehat{\mathcal{L}}^{(2)}_{\pi N} + \widehat{\mathcal{L}}^{(3)}_{\pi N} + \ldots \quad . \tag{1}$$

The pion isotriplet field $\vec{\Phi}$ is represented by the field $u(x)$ or $U(x)$, where $U = u^2$. In the so-called sigma para-

* Work supported in part by VEGA (Slovakia) grant No. 1/1323/96 and by FWF (Austria), Project No. P09505-PHY

Table 1. The field monomials P_i in $\mathcal{L}_{\pi\pi}^{(4)}$ contribu ting to the elastic πN scattering

i	P_i	γ_i
1	$4\left\langle u\cdot u\right\rangle^2$	1/3
2	$4\left\langle u^\mu u^\nu\right\rangle\left\langle u_\mu u_\nu\right\rangle$	2/3
3	$\left\langle\chi_+\right\rangle^2$	−1/2
4	$2\left\langle\chi_+\right\rangle\left\langle u\cdot u\right\rangle+2\left\langle\chi_-^2\right\rangle-\left\langle\chi_-\right\rangle^2$	2

metrization

$$U(x)=\sqrt{1-\frac{\vec{\Phi}^2(x)}{F^2}}+i\frac{\vec{\tau}\cdot\vec{\Phi}(x)}{F} \tag{2}$$

where $\vec{\tau}$ are Pauli matrices and F is a LEC of the meson Lagrangian $\mathcal{L}_{\pi\pi}^{(2)}$ (pion decay constant in the chiral limit). The nucleon isodoublet field $\Psi=\binom{p}{n}$ is decomposed using a time-like unit 4-vector v

$$\begin{aligned}N_v(x)&=\exp[imv\cdot x]P_v^+\Psi(x)\\H_v(x)&=\exp[imv\cdot x]P_v^-\Psi(x)\\P_v^\pm&=\tfrac{1}{2}(1\pm\not v)\ ,\qquad v^2=1\end{aligned} \tag{3}$$

(where m is the nucleon mass in the chiral limit) and the "heavy component" H_v is integrated out [12].

The Lagrangian (1) was constructed from the following building blocks:

$$\begin{aligned}u_\mu&=i\{u^\dagger(\partial_\mu-ir_\mu)u-u(\partial_\mu-i\ell_\mu)u^\dagger\}\\\Gamma_\mu&=\tfrac{1}{2}\{u^\dagger(\partial_\mu-ir_\mu)u+u(\partial_\mu-i\ell_\mu)u^\dagger\}\\\chi_\pm&=2B\{u^\dagger(s+ip)u^\dagger\pm u(s+ip)^\dagger u\}\\\nabla_\mu&=\partial_\mu+\Gamma_\mu-iv_\mu^{(s)}\\&\ \vdots\end{aligned} \tag{4}$$

where B is a LEC of the meson Lagrangian $\mathcal{L}_{\pi\pi}^{(2)}$ and s, p, ℓ_μ, r_μ, $v_\mu^{(s)}$ are external fields (scalar and pseudoscalar, left-handed and right-handed vector isotriplet and vector isosinglet, respectively). For the elastic πN scattering one can set these fields to zero (dots correspond to terms vanishing in such a case) with the only exception of the scalar field. Via this field the nonzero quark masses are taken into account, and in the isospin limit[1] $m_u=m_d$ one has [2]

$$2Bs=M^2 \tag{5}$$

where M is the bare pion mass.

[1] From now on we shall work within the isospin limit, without stating it always explicitly

Table 2. The field monomials O_i in $\widehat{\mathcal{L}}_{\pi N}^{(3)}$ contributing to the elastic πN scattering

i	O_i	β_i
1	$i[u_\mu,[v\cdot\nabla,u^\mu]]$	$-\dot{g}_A^4/6$
2	$i[u_\mu,[\nabla^\mu,v\cdot u]]$	$-(1+5\dot{g}_A^2)/12$
3	$i[v\cdot u,[v\cdot\nabla,v\cdot u]]$	$(3+\dot{g}_A^4)/6$
4	$i\langle u_\mu v\cdot u\rangle\nabla^\mu+\text{h.c.}$	0
6	$[\chi_-,v\cdot u]$	$(1+5\dot{g}_A^2)/24$
15	$\varepsilon^{\mu\nu\rho\sigma}v_\rho S_\sigma\langle[v\cdot\nabla,u_\mu]u_\nu\rangle$	$\dot{g}_A^4/3$
16	$\varepsilon^{\mu\nu\rho\sigma}v_\rho S_\sigma\langle u_\mu[\nabla_\nu,v\cdot u]\rangle$	0
17	$S\cdot u\langle\chi_+\rangle$	$\dot{g}_A/2+\dot{g}_A^3$
19	$iS^\mu[\nabla_\mu,\chi_-]$	0

Particular terms in (1) are [3][13]

$$\mathcal{L}_{\pi\pi}^{(2)}=\tfrac{F^2}{4}\left\langle u\cdot u+\chi_+\right\rangle$$

$$\mathcal{L}_{\pi\pi}^{(4)}=\tfrac{1}{16}\textstyle\sum_i l_iP_i$$

$$\widehat{\mathcal{L}}_{\pi N}^{(1)}=\bar{N}_v\left(iv\cdot\nabla+\dot{g}_AS\cdot u\right)N_v$$

$$\begin{aligned}\widehat{\mathcal{L}}_{\pi N}^{(2)}=\bar{N}_v\tfrac{1}{m}\Big(&-\tfrac{1}{2}(\nabla\cdot\nabla+i\dot{g}_A\{S\cdot\nabla,v\cdot u\})+a_1\langle u\cdot u\rangle\\&+a_2\langle(v\cdot u)^2\rangle+a_3\langle\chi_+\rangle\\&+a_5i\varepsilon^{\mu\nu\rho\sigma}v_\rho S_\sigma u_\mu u_\nu+\ldots\Big)N_v\end{aligned} \tag{6}$$

$$\begin{aligned}\widehat{\mathcal{L}}_{\pi N}^{(3)}=\bar{N}_v\Bigg(&\tfrac{\dot{g}_A}{8m^2}[\nabla_\mu,[\nabla^\mu,S\cdot u]]+\tfrac{1}{2m^2}\Big[\Big(a_5-\tfrac{1-3\dot{g}_A^2}{8}\Big)\\&\times i\varepsilon^{\mu\nu\rho\sigma}u_\mu u_\nu S_\sigma i\nabla_\rho+\tfrac{\dot{g}_A}{2}S\cdot\nabla\ u\cdot\nabla\\&+\tfrac{\dot{g}_A^2}{8}\{v\cdot u,u_\mu\}i\varepsilon^{\mu\nu\rho\sigma}v_\rho S_\sigma i\nabla_\nu+\text{h.c.}\Big]\\&+\tfrac{1}{(4\pi F)^2}\textstyle\sum_i b_iO_i+\ldots\Bigg)N_v\end{aligned}$$

where $S_\mu=\frac{i}{2}\gamma_5\sigma_{\mu\nu}v^\nu$ is the spin matrix, $\dot{g}_A$ is the neutron decay constant in the chiral limit, $\langle.\rangle$ denotes trace, and dots correspond to terms not contributing to the elastic πN scattering in the isospin limit. The field monomials P_i and O_i together with their γ_i and β_i (defined below) are collected in Tables 1 and 2.

Some of the LECs are divergent and are decomposed in the standard way (using dimensional regularization) as

$$\begin{aligned}l_i&=l_i^r(\mu)+\gamma_iL(\mu)\\b_i&=b_i^r(\mu)+(4\pi)^2\beta_iL(\mu)\end{aligned} \tag{7}$$

where

$$L(\mu)=\frac{\mu^{D-4}}{(4\pi)^2}\left\{\frac{1}{D-4}-\frac{1}{2}[\ln 4\pi+1+\Gamma'(1)]\right\}\quad. \tag{8}$$

The scale dependence of $l_i^r(\mu)$ and $b_i^r(\mu)$ is given by

$$\begin{aligned}l_i^r(\mu)&=l_i^r(\mu_0)+\tfrac{\gamma_i}{(4\pi)^2}\ln\tfrac{\mu_0}{\mu}\\b_i^r(\mu)&=b_i^r(\mu_0)+\beta_i\ln\tfrac{\mu_0}{\mu}\quad.\end{aligned} \tag{9}$$

In what follows we shall often use $\mu_0=M_\pi$ and express results in terms of $\bar{l}_i$ and $\widetilde{b}_i$ defined by

$$\begin{aligned}l_i^r(\mu)&=\tfrac{\gamma_i}{(4\pi)^2}\left(\tfrac{\bar{l}_i}{2}+\ln\tfrac{M_\pi}{\mu}\right)\\b_i^r(\mu)&=\widetilde{b}_i+\beta_i\ln\tfrac{M_\pi}{\mu}\quad.\end{aligned} \tag{10}$$

Finally let us note that the nucleon field N_v used in (6) is not exactly the one defined in (3), but is rather obtained from (3) by so-called EOM (equation of motion) transformations [13]. However, these EOM transformations have no effect on S-matrix elements.

2.2 Renormalization

To express the bare constants in $\mathcal{L}^{(2)}_{\pi\pi}$ and $\widehat{\mathcal{L}}^{(1)}_{\pi N}$ in terms of measurable quantities, one has to calculate one loop corrections (using these lowest order Lagrangians) to the pion and nucleon propagators, as well as to the coupling of the external axial field $a^\mu = (r^\mu - \ell^\mu)/2$ to a pion and to two nucleons. Tree contributions from the higher-order Lagrangians should be included as well. The results for pions are

$$\begin{aligned} M^2 &= M_\pi^2 \left(1 + \tfrac{M_\pi^2}{32\pi^2 F_\pi^2} \bar{l}_3\right) \\ Z_\pi &= 1 - \tfrac{M_\pi^2}{F_\pi^2}\left(2l_4^r + 6L(\mu) + \tfrac{1}{8\pi^2}\ln\tfrac{M_\pi}{\mu}\right) \\ F &= F_\pi\left(1 - \tfrac{M_\pi^2}{16\pi^2 F_\pi^2}\bar{l}_4\right) \end{aligned} \tag{11}$$

and for a nucleon with momentum $mv + k$

$$\begin{aligned} m &= m_N - \delta m \\ Z_N(k) &= 1 - \tfrac{\delta m}{m_N} + \tfrac{(k-\delta m.v)^2}{4m_N^2} \\ &\quad - \tfrac{3g_A^2 M_\pi^2}{4F_\pi^2}\left(6L(\mu) + \tfrac{1}{8\pi^2} + \tfrac{3}{8\pi^2}\ln\tfrac{M_\pi}{\mu}\right) \\ \dot{g}_A &= g_A\left(1 + \tfrac{\delta m}{m_N}\right) + \tfrac{M_\pi^2}{16\pi^2 F_\pi^2}\left(g_A^3 - 4\widetilde{b}_{17}\right) \end{aligned} \tag{12}$$

where

$$\delta m = -\frac{4M_\pi^2}{m_N} a_3 - \frac{3g_A^2 M_\pi^3}{32\pi F_\pi^2} \quad . \tag{13}$$

Let us comment on the results for nucleons, since they are different from what was used in most of previous calculations (see e.g. [14]). The first difference is the term $\delta m/m_N$ in Z_N-factor and $\dot{g}_A$. The reason of this difference is, as pointed out in [15], that the Lagrangian commonly used in previous calculations contains some terms, which were transformed away in (6) by EOM transformations [13]. The second difference is the term $(k - \delta m.v)^2/4m_N$ in Z_N-factor, which accounts for the contribution of heavy component of the nucleon source. This issue was not discussed in the literature on HBCHPT yet, so we shall briefly comment on it. More systematic analysis is to be found in [16].

In the path integral derivation of HBCHPT Lagrangian [12], one starts from the generating functional of Green functions with at most two nucleons

$$Z[\eta,\overline{\eta}] = \int \left[\mathcal{D}\Psi\mathcal{D}\overline{\Psi}\mathcal{D}u\right] \exp i \left\{ S_{\pi\pi} + S_{\pi N} + \int d^4x \ \left(\overline{\eta}\Psi + \overline{\Psi}\eta\right) \right\} \quad . \tag{14}$$

After decomposition of the nucleon field to heavy and light component (3) and similar decomposition of the nucleon source

$$\begin{aligned} \rho_v(x) &= \exp[imv\cdot x]P_v^+\eta(x) \\ R_v(x) &= \exp[imv\cdot x]P_v^-\eta(x) \end{aligned} \tag{15}$$

one writes

$$S_{\pi N} = \int d^4x \ \left\{\overline{N}_v A N_v + \overline{H}_v B N_v + \overline{N}_v B' H_v - \overline{H}_v C H_v\right\} \tag{16}$$

where $B' = \gamma^0 B^\dagger \gamma^0$. After Gaussian integration over $\left[\mathcal{D}H_v\mathcal{D}\overline{H}_v\right]$ one gets

$$\begin{aligned} Z[\rho_v, R_v, \overline{\rho}_v, \overline{R}_v] &= \int \left[\mathcal{D}N\mathcal{D}\overline{N}\mathcal{D}u\right] \ \Delta_H \\ &\quad \times \exp i\left\{S_{\pi\pi} + \widehat{S}_{\pi N} + \text{sources}\right\} \\ \widehat{S}_{\pi N} &= \int d^4x \ \widehat{\mathcal{L}}_{\pi N} = \int d^4x \ \overline{N}_v \left(A + B'C^{-1}B\right) N_v \\ \text{sources} &= \int d^4x \ \left[\left(\overline{\rho}_v + \overline{R}_v C^{-1}B\right) N_v \right. \\ &\quad \left. + \overline{N}_v\left(\rho_v + B'C^{-1}R_v\right) + \overline{R}_v C^{-1} R_v\right] \end{aligned} \tag{17}$$

where the determinant Δ_H turns out to be just a constant.

In S-matrix elements, the source η is, so to say, replaced by a Dirac bispinor $u(mv + k, \sigma)$ (for a nucleon with momentum $mv + k$ and spin σ) . The corresponding light and heavy components lead to

$$\begin{aligned} \rho_v &\to P_v^+ u(mv+k,\sigma) \\ &= \left(1 + \frac{\delta m}{2m_N}\not{v} - \frac{1}{2m_N}\not{k}\right) u(mv+k,\sigma) \\ R_v &\to P_v^- u(mv+k,\sigma) \\ &= \left(-\frac{\delta m}{2m_N}\not{v} + \frac{1}{2m_N}\not{k}\right) u(mv+k,\sigma) \quad . \end{aligned} \tag{18}$$

Clearly, ρ_v leads to a quantity of the zeroth, and R_v of the first chiral order. The lowest chiral order in the products $C^{-1}B$ and $B'C^{-1}$ is also the first one. So the heavy source terms in (17) contribute two chiral orders higher than the light source ones, and they start to contribute at the third chiral order.

To incorporate heavy sources into calculations of various amplitudes does not require any extra effort. For every Feynman diagram with light sources, one just adds diagrams with one or both light sources replaced by the heavy ones - the only differences in corresponding amplitudes are different factors for nucleon external legs. As a matter of fact, the whole effect of heavy sources is finally reduced to the momentum dependent, but otherwise very simple term in Z_N-factor. Using Z_N given by (12), one can calculate with just light sources and forget completely about heavy ones, since all their effect is taken into account in this Z_N [16].

Heavy sources were not considered explicitly in most of previous calculations. The reason is that in the third order they only appear as the Z_N corrections to the first order, and the first order used to be treated in a special way – namely one used the original "relativistic" Lagrangian

$\mathcal{L}^{(1)}_{\pi N}$ and then expanded the result in $\mu = M_\pi/m_N$. Advantage of this approach is that it gives automatically not only the lowest order amplitude, but also higher order corrections to it, including the discussed part of the Z_N correction. Disadvantage, from our point of view, is that part of these higher order corrections is included in the definition of LECs of higher orders. So to avoid double counting in "relativistic 1-st order" approach, one has to know precisely what portion of LECs comes from the lowest order Lagrangian. This is well known for the second order LECs, but not for the third order ones, and if one does not want to work this out, it is better to perform the whole calculation strictly within HBCHPT.

However, we can use "relativistic 1-st order" approach to check our prescription for the treatment of heavy sources. Let us take e.g. Born term for the elastic πN-scattering (i.e. first order term with the nucleon propagator). "Relativistic 1-st order" calculation gives for the invariant amplitude A^+ defined below in (35)

$$A^+_{rel} = \frac{g_A^2 m_N}{F_\pi^2} \quad . \tag{19}$$

On the other hand, HBCHPT calculation of the same term in tree approximation up to the third order, ignoring heavy sources and expanding in μ, gives (for a kinematics defined by (23), (27))

$$A^+ = \frac{g_A^2}{F_\pi^2}\left(m_N - \frac{t}{8m_N}\right) + \ldots \tag{20}$$

and heavy source contribution, which turns out to give just an overall multiplicative factor $\left(1 + t/8m_N^2\right)$, brings these two results in agreement. For the invariant amplitude B^+ one has the same situation, since also here one gets

$$B^+ = B^+_{rel}\left(1 - \frac{t}{8m_N^2}\right) + \ldots \quad . \tag{21}$$

For the invariant amplitudes A^- and B^-, "relativistic 1-st order" and HBCHPT results agree to order $\mathcal{O}(\mu^2)$ even without heavy sources contribution, and this agreement is not spoiled by the heavy sources correction, because it starts to contribute only at order $\mathcal{O}(\mu^3)$.

3 Elastic πN scattering

3.1 Kinematics

For the elastic πN scattering we use the following kinematics: ingoing pion with momentum q and isospin a, outgoing pion with momentum q' and isospin b, ingoing nucleon with momentum $mv + p$, and outgoing nucleon with momentum $mv + p'$

$$\pi^a(q) + N(mv + p) \to \pi^b(q') + N(mv + p') \quad . \tag{22}$$

The natural (and advantageous) choice for the 4-vector v is the 4-velocity of the ingoing (on-shell) nucleon

$$m_N v = mv + p \quad . \tag{23}$$

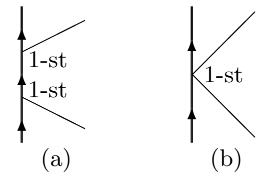

Fig. 1. Feynman diagrams for πN scattering contributing to the first chiral order. *Thick* and *thin lines* correspond to nucleons and pions, respectively. Crossed diagrams are not shown

In such a case one has $p = \delta m.v$, where δm is the sum of small quantities of the second and third orders, and so p itself is also a small quantity of the second order.

The scattering amplitude T is given in the form

$$T = T^+\delta^{ab} - T^- i\varepsilon^{abc}\tau^c$$
$$T^\pm = \overline{u}_N(p',\sigma')\left(\alpha^\pm + \beta^\pm i\varepsilon^{\mu\nu\rho\omega} q_\mu q'_\nu v_\rho S_\omega\right) u_N(p,\sigma) \quad . \tag{24}$$

where

$$\begin{aligned} u_N(p,\sigma) &= P_v^+ u(mv+p,\sigma) = u(mv+p,\sigma) \\ u_N(p',\sigma') &= P_v^+ u(mv+p',\sigma') \\ &= \left[1 + \tfrac{1}{2m_N}(\not{p} - \not{p}')\right] u(mv+p',\sigma') \quad . \end{aligned} \tag{25}$$

The kinematics enables a significant simplification in the highest order (third one in our case) of the chiral expansion of the scattering amplitude. It is based on the fact that for the on-shell outgoing nucleon, $v \cdot p'$ is of the chiral order 2 (although $p' = p + q - q'$ itself is of the chiral order 1).

$$\begin{aligned} m_N^2 = (mv + p')^2 \quad \Rightarrow \quad v \cdot p' &= \frac{m_N^2 - m^2}{2m} - \frac{p'^2}{2m} \\ &= \mathcal{O}(p^2)\,. \end{aligned} \tag{26}$$

So one can neglect $v \cdot p'$ (as well as $v \cdot p$) in the highest-order amplitude. Or in other words, one can replace every $v \cdot q'$ by $v \cdot q$ in the highest-order. The error thus introduced is of even higher chiral order, beyond the level of precision of the calculation at hand.

For sake of brevity, the following notation is used $w \equiv v \cdot q$, $w' \equiv v \cdot q'$ and if needed, one can express the amplitude in the usual Mandelstam variables $s = (m_N v + q)^2$, $t = (q - q')^2$ and $u = (m_N v - q')^2$ using

$$\begin{aligned} q \cdot q' &= M_\pi^2 - \tfrac{t}{2} \\ v \cdot q &= \tfrac{1}{2m_N}\left(s - m_N^2 - M_\pi^2\right) \\ v \cdot q' &= \tfrac{1}{2m_N}\left(s - m_N^2 - M_\pi^2 + t\right) \quad . \end{aligned} \tag{27}$$

3.2 Scattering amplitude

We shall present the amplitude order by order in the chiral expansion

$$T = T_{(1)} + T_{(2)} + T_{(3)} \quad . \tag{28}$$

$T_{(1)}$ is given by the tree graphs (Fig. 1) containing vertices defined by $\widehat{\mathcal{L}}^{(1)}_{\pi N}$ (labelled as "1-st" in Figs. 1–3),

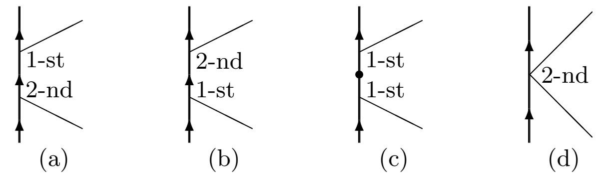

Fig. 2. Diagrams contributing to the second chiral order. *Black circle* is the second order counterterm. Crossed diagrams are not shown

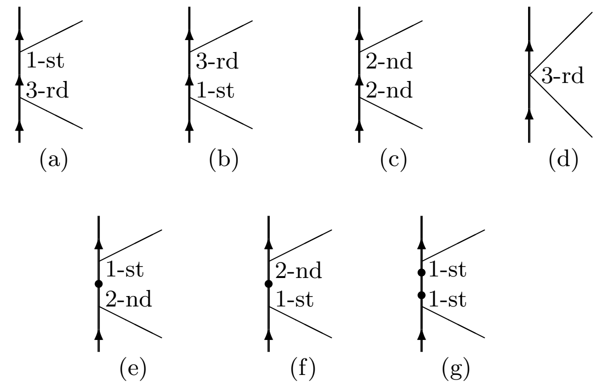

Fig. 3. Tree diagrams contributing to the third chiral order. Crossed diagrams are not shown

with the bare coupling constants and masses (F, $\dot{g}_A$, M and m) replaced by their physical values (F_π, g_A, M_π and m_N) in the final formulae. This replacement (which will take place in all orders $T_{(n)}$) just means that after writing $F = F_\pi - \delta F_\pi$, etc. and expanding into a power series in the deltas (δF_π, etc.), we keep in the given order of the chiral expansion only the lowest order in deltas, higher orders in deltas are incorporated into higher orders of the chiral expansion. (The reason for this standard procedure is that it guarantees exactly the same form of $T_{(1)}$ in tree calculation, one-loop calculation, etc., and an analogous statement is true for any higher $T_{(n)}$.)

$T_{(2)}$ is given by the tree graphs with one vertex from $\widehat{\mathcal{L}}^{(2)}_{\pi N}$ (labelled as "2-nd" in Figs. 1–3) and all the other vertices from $\widehat{\mathcal{L}}^{(1)}_{\pi N}$ (Fig. 2). Again the bare coupling constants and masses are replaced by their physical values.

Finally, $T_{(3)}$ is given by the sum $T^{\rm tree}_{(3)} + T^{\rm loop}_{(3)} + T^{\delta}_{(3)}$. Here $T^{\rm tree}_{(3)}$ is given by the tree graphs with either one vertex from $\widehat{\mathcal{L}}^{(3)}_{\pi N}$ (labelled as "3-rd" in Figs. 1–3) or two vertices from $\widehat{\mathcal{L}}^{(2)}_{\pi N}$, and all the other vertices from $\widehat{\mathcal{L}}^{(1)}_{\pi N}$ (Fig. 3). The loop contribution $T^{\rm loop}_{(3)}$ is given by one-loop graphs with vertices from $\widehat{\mathcal{L}}^{(1)}_{\pi N} + \mathcal{L}^{(2)}_{\pi\pi}$ (Fig. 4). As always, the bare constants are replaced by their physical values. The third term $T^{\delta}_{(3)}$ is just the contribution from this replacement in lower orders.

Both $T^{\rm tree}_{(3)}$ and $T^{\rm loop}_{(3)}$ are infinite and renormalization scale dependent. It is preferable to have the result in the explicitly finite and renormalization scale independent form, so we shall shift all the infinite and μ-dependent terms from $T^{\rm loop}_{(3)}$ to $T^{\rm tree}_{(3)}$. These shifted terms are polynomials in external momenta (otherwise they could not be canceled by the counterterms from $\widehat{\mathcal{L}}^{(3)}_{\pi N}$) and it is reasonable to shift from $T^{\rm loop}_{(3)}$ to $T^{\rm tree}_{(3)}$ also other possible polynomial terms (in external momenta, including terms with negative powers of w), so that after adding also $T^{\delta}_{(3)}$ to $T^{\rm tree}_{(3)}$, one has a clear separation of the amplitude into the part $T^{\rm pol}_{(3)}$, polynomial in external momenta plus poles in w, and the rest $T^{\rm uni}_{(3)}$, which contains imaginary part, required by unitarity.

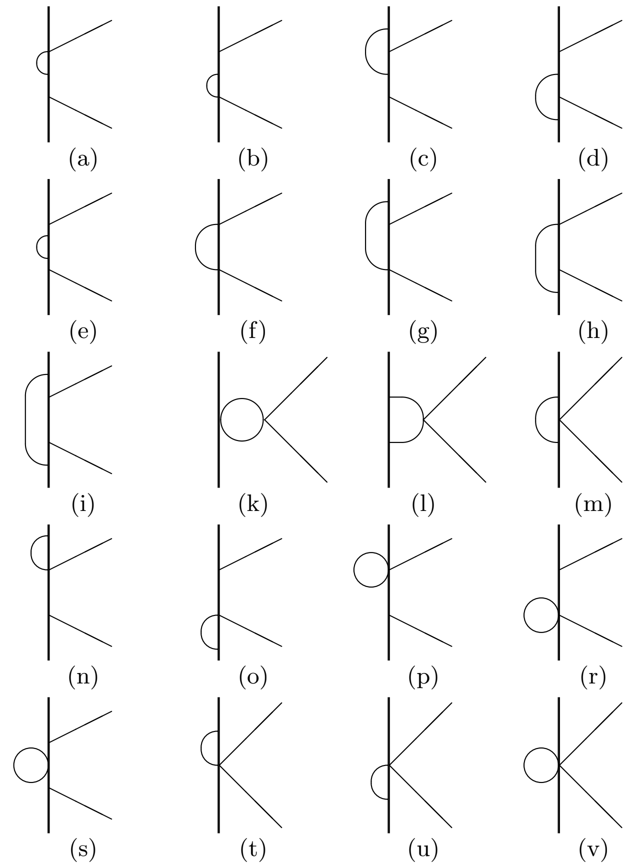

Fig. 4. 1-loop diagrams contributing to the third chiral order. Crossed diagrams are not shown

We shall therefore present results at the third order in the form

$$T_{(3)} = T^{\rm pol}_{(3)} + T^{\rm uni}_{(3)} \quad . \tag{29}$$

$T^{\rm uni}_{(3)}$ is made finite and scale independent by hand, $T^{\rm pol}_{(3)}$ by the cancellations of divergent and scale dependent terms from loops and counterterms. The counterterms in the third-order Lagrangian (Table 2) were completely fixed by the general renormalization of the generating functional [17], and so this cancellation provides us with a nontrivial check of the calculations.

Calculation of T from (1) is in principle straightforward. Here we present just the final result, details are postponed to Appendix C. For loop functions the following notation is used

$$\begin{aligned}
J_{\pm}^{\mathrm{uni}}(w) &= J_0^{\mathrm{uni}}(w) \pm J_0^{\mathrm{uni}}(-w)\\
J_0^{\mathrm{uni}}(w) &= J_0(w) + 4wL(\mu) - \tfrac{w}{8\pi^2}\left(1 - 2\ln\tfrac{M}{\mu}\right)\\
I_0^{\mathrm{uni}}(t) &= I_0(t) + 2L(\mu) - \tfrac{1}{16\pi^2}\left(1 - 2\ln\tfrac{M}{\mu}\right)
\end{aligned} \tag{30}$$

and the loop integrals I_0, J_0, and K_0 (which will appear later) are displayed in Appendix B. All the loop integrals in the amplitude are understood with the bare pion mass M replaced by the physical mass M_π.

Let us remark that two of the LECs from Table 2 – namely b_4 and b_{17} – do not appear in the result. The reason for b_4 is that the term containing this LEC is of the form $w\, p\cdot(q+q')$ which is of the fourth chiral order, since p itself is of the second order for the on-shell nucleon. The reason for b_{17} is, on the other hand, cancellation (in the third order) of different terms containing this LEC. All the other LECs from Table 2 are present in the result given below[2]:

$$\alpha^+_{(1)} = \tfrac{g_A^2}{4F_\pi^2}\left(\tfrac{1}{w} - \tfrac{1}{w'}\right)\left(q\cdot q' - ww'\right)$$

$$\begin{aligned}
\alpha^+_{(2)} &= \tfrac{4}{m_N F_\pi^2}\left(a_1 q\cdot q' + a_2\, ww' - a_3 M_\pi^2\right)\\
&+ \tfrac{g_A^2}{8m_N F_\pi^2}\Big[\left(\tfrac{1}{w^2} + \tfrac{1}{w'^2}\right)\\
&\times\left(ww' q\cdot q' - M_\pi^2 ww' - M_\pi^2 q\cdot q' - w^2 w'^2\right)\\
&+ 6ww' - 2q\cdot q'\Big]
\end{aligned} \tag{31}$$

$$\alpha^{+\,\mathrm{pol}}_{(3)} = \tfrac{g_A^2 M_\pi}{32\pi F_\pi^4}\left(4q\cdot q' - 3M_\pi^2\right) + \tfrac{g_A^4 M_\pi^3}{12\pi F_\pi^4}\tfrac{1}{w^2}\left(q\cdot q' - w^2\right)$$

$$\begin{aligned}
\alpha^{+\,\mathrm{uni}}_{(3)} &= \tfrac{1}{2F_\pi^4} w^2 J_+^{\mathrm{uni}}(w)\\
&- \tfrac{g_A^2}{8F_\pi^4}\left(2M_\pi^2 - t\right)\left(M_\pi^2 - 2t\right) K_0(0,t)\\
&+ \tfrac{g_A^4}{3F_\pi^4}\tfrac{1}{w^2}\left(q\cdot q' - w^2\right)\left(M_\pi^2 - w^2\right) J_+^{\mathrm{uni}}(w)
\end{aligned}$$

$$\beta^+_{(1)} = \tfrac{g_A^2}{2F_\pi^2}\left(\tfrac{1}{w} + \tfrac{1}{w'}\right)$$

$$\beta^+_{(2)} = \tfrac{g_A^2}{4m_N F_\pi^2}\left(\tfrac{1}{w^2} - \tfrac{1}{w'^2}\right)\left(ww' - M_\pi^2\right)$$

$$\begin{aligned}
\beta^{+\,\mathrm{pol}}_{(3)} &= \tfrac{1}{4\pi^2 F_\pi^4}\left[\left(b_{16} - \widetilde{b}_{15}\right) w - b_{19}\tfrac{g_A M_\pi^2}{w}\right]\\
&+ \tfrac{g_A^2 M_\pi^4}{4m_N^2 F_\pi^2}\tfrac{1}{w^3} + \tfrac{g_A^4}{72\pi^2 F_\pi^4}\tfrac{1}{w}\left(w^2 + 6M_\pi^2\right)
\end{aligned} \tag{32}$$

$$\beta^{+\,\mathrm{uni}}_{(3)} = \tfrac{g_A^4}{6F_\pi^4}\tfrac{1}{w^2}\left(M_\pi^2 - w^2\right) J_-^{\mathrm{uni}}(w)$$

$$\alpha^-_{(1)} = \frac{g_A^2}{4F_\pi^2}\left(\frac{1}{w} + \frac{1}{w'}\right)\left(q\cdot q' - ww'\right) + \frac{1}{4F_\pi^2}\left(w + w'\right)$$

$$\begin{aligned}
\alpha^-_{(2)} &= \tfrac{g_A^2}{8m_N F_\pi^2}\left(\tfrac{1}{w^2} - \tfrac{1}{w'^2}\right)\Big(ww' q\cdot q' - M_\pi^2 ww'\\
&\quad - M_\pi^2 q\cdot q' - w^2 w'^2\Big)
\end{aligned}$$

$$\begin{aligned}
\alpha^{-\,\mathrm{pol}}_{(3)} &= \tfrac{1}{4\pi^2 F_\pi^4} w\Big[\left(\widetilde{b}_1 + \widetilde{b}_2\right) q\cdot q' + \widetilde{b}_3 w^2 + 2\widetilde{b}_6 M_\pi^2\\
&\quad - b_{19}\tfrac{g_A M_\pi^2}{2w^2}\left(q\cdot q' - w^2\right)\Big]\\
&+ \tfrac{g_A^2 M_\pi^2}{8m_N^2 F_\pi^2}\tfrac{1}{w}\Big\{\left(q\cdot q' - w^2\right)\left[1 + \tfrac{M_\pi^2}{w^2} + \tfrac{w^2}{M_\pi^2}\right]\\
&\quad + 3\left(M_\pi^2 - q\cdot q'\right)\Big\}\\
&+ \tfrac{1}{288\pi^2 F_\pi^4} w\Big[18w^2 - \left(7 + 11g_A^2\right) M_\pi^2\\
&\quad - \left(5 + 13g_A^2\right) q\cdot q'\Big]\\
&+ \tfrac{g_A^4}{144\pi^2 F_\pi^4}\tfrac{1}{w}\left(q\cdot q' - w^2\right)\left(6M_\pi^2 - 5w^2\right)\\
&+ \tfrac{2}{m_N^2 F_\pi^2} w\left(M_\pi^2 a_3 + \tfrac{1}{32} t\right)
\end{aligned} \tag{33}$$

$$\begin{aligned}
\alpha^{-\,\mathrm{uni}}_{(3)} &= \tfrac{1}{12F_\pi^4}\Big[3w^2 + g_A^4\tfrac{1}{w^2}(q\cdot q' - w^2)\\
&\quad\times(M_\pi^2 - w^2)\Big] J_-^{\mathrm{uni}}(w)\\
&- \tfrac{1}{3F_\pi^4} w\left[\left(M_\pi^2 - \tfrac{1}{4}t\right) + 2g_A^2\left(M_\pi^2 - \tfrac{5}{8}t\right)\right] I_0^{\mathrm{uni}}(t)
\end{aligned}$$

$$\beta^-_{(1)} = \tfrac{g_A^2}{2F_\pi^2}\left(\tfrac{1}{w} - \tfrac{1}{w'}\right)$$

$$\begin{aligned}
\beta^-_{(2)} &= -\tfrac{2}{m_N F_\pi^2} a_5\\
&+ \tfrac{g_A^2}{4m_N F_\pi^2}\left[\left(\tfrac{1}{w^2} + \tfrac{1}{w'^2}\right)\left(ww' - M_\pi^2\right) - 2\right]
\end{aligned} \tag{34}$$

$$\beta^{-\,\mathrm{pol}}_{(3)} = \tfrac{g_A^2 M_\pi}{16\pi F_\pi^4} + \tfrac{g_A^4 M_\pi^3}{12\pi F_\pi^4}\tfrac{1}{w^2}$$

$$\begin{aligned}
\beta^{-\,\mathrm{uni}}_{(3)} &= \tfrac{g_A^2}{4F_\pi^4}\left(t - 4M_\pi^2\right) K_0(0,t)\\
&+ \tfrac{g_A^4}{3F_\pi^4}\tfrac{1}{w^2}(M_\pi^2 - w^2) J_+^{\mathrm{uni}}(w)\,.
\end{aligned}$$

4 Comparison with data

4.1 Partial waves and threshold parameters

To compare with experiment, it is convenient to express the results in terms of $A^\pm$ and $B^\pm$, defined by the standard parametrization of the elastic πN scattering amplitude

$$\begin{aligned}
T^\pm_{\pi N} &= \overline{u}(mv + p', \sigma')\left[A^\pm(s,t,u) + B^\pm(s,t,u)\frac{\not q + \not q'}{2}\right]\\
&\quad\times u(mv + p, \sigma)\,.
\end{aligned} \tag{35}$$

Starting from (25) one derives (after some algebra) following relations between $\alpha^\pm$, $\beta^\pm$ and $A^\pm$, $B^\pm$ (see also [16])

$$\begin{aligned}
A^\pm &= \left(\alpha^\pm + \tfrac{s-u}{4}\beta^\pm\right)\\
B^\pm &= \left(-m_N + \tfrac{t}{4m_N}\right)\beta^\pm \quad .
\end{aligned} \tag{36}$$

Experimental information about elastic πN-scattering is usually given in terms of partial waves. For low energies, partial waves are characterized by a small number of

[2] For sake of completeness let us note that when taking into account also isospin breaking effects, three more LECs would appear, namely a_4, b_{18} and b_{20}

Table 3. Comparison of the HBCHPT results for two D-wave and four F-wave threshold parameters up to the first, second and third order, with (extrapolated) experimental values. Units for D-wave are GeV^{-5}, for F-wave they are GeV^{-7}

	up to $\mathcal{O}(p)$	up to $\mathcal{O}(p^2)$	up to $\mathcal{O}(p^3)$	**exp.**
a^+_{2+}	-55	-59	-36	-36 ± 7
a^-_{2+}	55	59	56	64 ± 3
a^+_{3+}	180	210	280	440 ± 140
a^+_{3-}	-30	-31	31	160 ± 120
a^-_{3+}	-180	-210	-210	-260 ± 20
a^-_{3-}	30	34	57	100 ± 20

threshold parameters such as scattering lengths, volumes, effective ranges, etc. These threshold parameters are not directly measurable, they can be extrapolated, however, from the experimental data above threshold [18][19]. Since the closer to threshold one is, the better CHPT is expected to work, these parameters seem to be the most suitable quantities to calculate and to compare with the (extrapolated) experimental values.

Partial wave amplitudes for the scattering of a spinless particle on a spin $\frac{1}{2}$ particle are given by [18]

$$\begin{aligned} f^\pm_{l\pm}(s) = \tfrac{1}{16\pi\sqrt{s}} \int_{-1}^{1} \{ & (E+m_N)[A^\pm(s,\theta) \\ & + (\sqrt{s}-m_N)B^\pm(s,\theta)]P_l(\cos\theta) \\ & - (E-m_N)[A^\pm(s,\theta) - (\sqrt{s}+m_N)B^\pm(s,\theta)] \\ & \times P_{l\pm 1}(\cos\theta)\}\, d\cos\theta \end{aligned} \quad (37)$$

where E is the nucleon energy in CMS, and θ is the scattering angle in CMS. The low-energy behavior of the partial wave amplitudes is characterized by the threshold parameters $a^\pm_{l\pm}$, $b^\pm_{l\pm}$ defined by the expansion

$$\mathrm{Re}\ f^\pm_{l\pm}(s) = a^\pm_{l\pm} k^{2l} + b^\pm_{l\pm} k^{2l+2} + \ldots \quad (38)$$

where $\vec{k}$ is the 3-momentum of a particle in CMS.

Calculation of these threshold parameters from the scattering amplitude (31–34) is in principle straightforward, results for the first four partial waves are given in Appendix D.

4.2 Threshold parameters independent of LECs a_i, b_j

The scattering amplitude (31–34), and therefore also the sixteen threshold parameters given in Appendix D, contain four LECs of the second-order πN Lagrangian (a_1, a_2, a_3, a_5) and five linear combinations of LECs of the third-order πN Lagrangian ($\widetilde{b}_1 + \widetilde{b}_2$, $\widetilde{b}_3$, $\widetilde{b}_6$, $b_{16} - \widetilde{b}_{15}$, b_{19}). However, six out of these sixteen threshold parameters do not depend on any of these LECs. So we have at our disposal six parameter-free (where by parameters the LECs a_i and b_j are understood) HBCHPT predictions.

To compare them with experimental data, one needs some consistent set of extrapolated threshold parameters, for which we take [20]. This comparison, which is shown in Table 3, is neither too impressive, nor discouraging.[3] Two main lessons can be drawn from Table 3:

Table 4. The values of LECs from the χ^2-fit to the 10 πN scattering threshold parameters, the nucleon σ-term, and the Goldberger-Treiman discrepancy. Uncertainities refer to the parabolic errors of the MINUIT routine

a_1	-2.60 ± 0.03
a_2	1.40 ± 0.05
a_3	-1.00 ± 0.06
a_5	3.30 ± 0.05
$\widetilde{b}_1 + \widetilde{b}_2$	2.4 ± 0.3
$\widetilde{b}_3$	-2.8 ± 0.6
$\widetilde{b}_6$	1.4 ± 0.3
$b_{16} - \widetilde{b}_{15}$	6.1 ± 0.6
b_{19}	-2.4 ± 0.4

– There is a clear improvement, when going from lower to higher orders of HBCHPT.
– Contributions of different orders are comparable, i.e. the chiral expansion converges slowly.

Our results for D- and F-wave threshold parameters are in agreement with independent calculation of these parameters in [10]. In this work the Born term was treated in different manner, namely the "relativistic 1-st order" approach (discussed above) was used and results are presented to the leading (F-waves) and next-to-leading (D-waves) order in powers of $\mu = M_\pi/m_N$. Our calculation, on the other hand, is fully based on the HBCHPT Lagrangian. For every threshold parameter, the two approaches give the same result to the order in powers of μ given in [10], but there are differences in higher orders of μ, leading in some cases to nonnegligible (but not at all dramatic) differences in numerical values of the threshold parameters.

4.3 Remaining threshold parameters and LECs a_i, b_j

Let us now turn our attention to the remaining ten threshold parameters. As mentioned above, they contain nine LECs a_i, b_j and/or their linear combinations. Two of them are present also in HBCHPT results for two other quantities closely related to πN scattering. The first one is the pion-nucleon σ-term

$$\sigma = \frac{1}{2m_N} \left\langle P \left| \widehat{m}(\overline{u}u + \overline{d}d) \right| P \right\rangle \quad (39)$$

where P is the nucleon 4-momentum, $\widehat{m} = (m_u + m_d)/2$ and u, d are quark fields. The second one is the Goldberger-Treiman discrepancy $1 - g_A m_N / F_\pi g_{\pi N}$. Up to the third order of HBCHPT [6]

[3] One should be aware that experimental errors in [20] are underestimated, since they refer "only to that part which can be estimated from deviations from the internal consistency of the method"

Table 5. HBCHPT predictions for the 10 elastic πN scattering threshold parameters up to the first, second and third order, compared with (extrapolated) experimental values. Theoretical uncertainties are shown only in the third order

	up to $\mathcal{O}(p)$	up to $\mathcal{O}(p^2)$	up to $\mathcal{O}(p^3)$	**exp.**	units
a_0^+	0	-0.13	-0.07 ± 0.09	-0.07 ± 0.01	GeV^{-1}
b_0^+	0	-24	-13.9 ± 3.0	-16.9 ± 2.5	GeV^{-3}
a_0^-	0.55	0.55	0.67 ± 0.10	0.66 ± 0.01	GeV^{-1}
b_0^-	7.2	8.2	5.5 ± 6.7	5.1 ± 2.3	GeV^{-3}
a_{1+}^+	17.6	51.2	50.4 ± 1.1	50.5 ± 0.5	GeV^{-3}
a_{1-}^+	-35.3	-1.7	-21.6 ± 1.8	-21.6 ± 0.5	GeV^{-3}
a_{1+}^-	-16.9	-29.3	-31.0 ± 0.8	-31.0 ± 0.6	GeV^{-3}
a_{1-}^-	-17.1	6.7	-4.5 ± 1.0	-4.4 ± 0.4	GeV^{-3}
a_{2-}^+	18.6	4.6	31.2 ± 0.3	44 ± 7	GeV^{-5}
a_{2-}^-	-8.8	-17.6	-5.0 ± 0.2	2 ± 3	GeV^{-5}

$$\sigma = -\frac{4M_\pi^2}{m_N} a_3 - \frac{9g_A^2 M_\pi^3}{64\pi F_\pi^2} \tag{40}$$

$$g_{\pi N} = g_A \frac{m_N}{F_\pi} \left(1 - \frac{M_\pi^2}{8\pi^2 F_\pi^2 g_A} b_{19}\right) \quad . \tag{41}$$

Values of the LECs can now be fixed by fitting the HBCHPT results to the (extrapolated) experimental values of the remaining ten threshold parameters, σ-term and $g_{\pi N}$. Results of such a procedure, using values $M_\pi =$ 138MeV, $m_N = 939$MeV, $F_\pi = 93$MeV, $g_A = 1.26, \sigma = 45 \pm 8$MeV, $g_{\pi N} = 13.4 \pm 0.1$ and threshold parameters from [20], are presented in Table 4. (Let us recall that values of $b_{16} - \widetilde{b}_{15}$ and b_{19} depend on the choice of mesonic Lagrangian $\mathcal{L}_{\pi\pi}^{(4)}$ [13].)

One should stress that errors given in Table 4 are probably too optimistic, as a consequence of probably too optimistic errors of the used (extrapolated) experimental values of the threshold parameters. Another consequence of these probably underestimated errors is the relatively large value of the σ-term, $\sigma = 59 \pm 5$ MeV (corresponding to $a_3 = -1.00 \pm 0.06$). Enhancing error bars of the threshold parameters leads to a value of σ-term closer to the experimental one. Another possibility, how to avoid a large σ-term, is to fix a_3 directly from the σ-term and not to treat it as free parameter in the fitting procedure. When doing so, it turns out that the third order LECs b_i are not sensitive to the precise value of the σ-term. Variation of a_3 from -0.8 to -1.0 (corresponding to variation of σ from 45 to 60 MeV) leaves the third order LECs almost untouched.

On the other hand, the third order LECs are sensitive to the value of $g_{\pi N}$. For $g_{\pi N} = 13.0 \pm 0.1$ one obtains $\widetilde{b}_1 + \widetilde{b}_2 = 3.3 \pm 0.3$, $\widetilde{b}_3 = -3.7 \pm 0.6$, $\widetilde{b}_6 = 1.4 \pm 0.3$, $b_{16} - \widetilde{b}_{15} = 7.9 \pm 0.6$ and $b_{19} = -1.0 \pm 0.4$.

The values of the second order LECs a_i are in good agreement with their recent determination [10] ($a_1 = -2.59 \pm 0.2$, $a_2 = 1.57 \pm 0.1$, $a_3 = -0.92 \pm 0.1$, $a_5 = 3.48 \pm 0.05$ in our conventions). These values were obtained from a fit to the σ-term and eight other observables, four of them being some linear combinations of the threshold parameters used in our fit and another four being subthreshold parameters, not used by us. So the agreement is not a trivial one. As a matter of fact, the quoted results of [10] were obtained in a fit with enhanced error bars for threshold and subthreshold parameters (for reasons mentioned above). Original error bars lead to $a_1 = -2.68 \pm 0.03$, $a_2 = 1.47 \pm 0.02$, $a_3 = -1.02 \pm 0.06$, in even better agreement with our results.

Table 6. Comparison of contributions from counterterms with third order LECs and contributions from loops + other counterterms (denoted together as "rest"). Comparison is made in the third order at the renormalization scale $\mu = 1$GeV. For the remaining 8 threshold parameters, not displayed in the Table, contributions from counterterms with third-order LECs vanish

	LECs	**rest**	units
a_0^-	0.09	0.03	GeV^{-1}
b_0^-	-3.3	0.5	GeV^{-3}
a_{1+}^+	6.7	-7.5	GeV^{-3}
a_{1-}^+	-13.4	-6.5	GeV^{-3}
a_{1+}^-	-6.7	5.1	GeV^{-3}
a_{1-}^-	-6.7	-4.5	GeV^{-3}
a_{2-}^+	1.9	24.7	GeV^{-5}
a_{2-}^-	1.9	10.8	GeV^{-5}

Once we have pinned down the LECs, we can compare explicitly our results for the threshold parameters with the values given in [20]. This is done, order by order, in Table 5.

At first sight, there is remarkable agreement between theory and experiment. This statement is however almost empty, since we have chosen the values of LECs just to obtain such an agreement. The nontrivial content of this agreement is that it was achieved with reasonable, i.e. not unnaturally large, values of LECs.

A criterion for the natural size of LECs is that corresponding counterterm contributions are not too large when compared to other contributions (loops and counterterms with fixed coefficients and/or lower order LECs) of the same order. Of course, such a comparison requires choosing some typical renormalization scale μ. Numerical results for $\mu = 1$GeV are presented in Table 6. Contributions of the counterterms with the third order LECs are comparable, or even considerably lower than the rest of the contributions to the third order.

Finally let us remark that both lessons learned from Table 3 are confirmed by Table 5 – the chiral expansion converges to the experimental values, but the convergence seems to be rather slow, in a sense that contributions to different orders are comparable. This fact seems to show that despite of the relative success in describing elastic πN scattering at threshold, the third order is definitely not the whole story. A complete 1-loop calculation, which will include the fourth order of the chiral expansion, is probably needed for sufficiently reliable description of this process.

5 Conclusions

We have calculated the elastic πN scattering amplitude in the isospin limit in the framework of HBCHPT, up to the third order. Since the chiral expansion is supposed to work well near threshold, we have used the extrapolated threshold parameters, like scattering lengths, volumes, effective ranges, etc., to compare the results with data.

The elastic πN scattering amplitude and therefore also the threshold parameters contain nine low energy constants (besides F_π and g_A from the lowest order Lagrangians). All these LECs were fixed from the available pion-nucleon data – the pion-nucleon σ-term, Goldberger-Treiman discrepancy and the threshold parameters. Values of the second order LECs are in a quite good agreement with their recent determination in [10]. Values of the third order LECs were not determined directly from πN data until now.

The third-order calculation brought a clear improvement in the description of data, and this improvement was achieved with naturally small LECs. The results, however, suggest importance of higher-order corrections, since the contributions of the first three orders are frequently comparable and this will probably be the case also in the fourth order.

A Feynman rules

Propagators and vertices used in the calculation of elastic πN-scattering are summarized. Most of them can be found, e.g., in [6], we present them here mainly for the sake of completeness and also because of slightly different notation. Rules are given in the isospin limit $m_u = m_d$. Nucleon momentum in final state p' is outgoing, all the other momenta are ingoing. Momenta and isospins of pions are denoted as $(q_1, a)\,,\,(q_2, b)\,,\,(q_3, c)\,,\,(q_4, d)\,.$

Propagators

pion propagator

$$\frac{i\delta_{ab}}{k^2 - M^2 + i\varepsilon} \tag{42}$$

nucleon propagator

$$\frac{i}{v\cdot p + i\varepsilon} \tag{43}$$

πN vertices from $\widehat{\mathcal{L}}^{(1)}_{\pi N}$

one pion

$$-\frac{\dot{g}_A}{F}\; S.q\;\tau_a \tag{44}$$

two pions

$$\frac{1}{4F^2}\; v.(q_1 - q_2)\;\varepsilon_{abc}\tau_c \tag{45}$$

three pions

$$-\frac{\dot{g}_A}{2F^3}\,[S.(q_1+q_2)\;\delta_{ab}\tau_c + S.(q_1+q_3)\;\delta_{ac}\tau_b + S.(q_2+q_3)\;\delta_{bc}\tau_a] \tag{46}$$

four pions

$$\begin{aligned}&\tfrac{i}{2F^4}\; v.(q_1+q_2+q_3+q_4)\;(\delta_{ab}\delta_{cd}+\delta_{ac}\delta_{bd}+\delta_{ad}\delta_{bc})\\ &-\tfrac{1}{8F^4}\;[v.(q_2-q_1)\;\delta_{cd}\varepsilon_{abf}\tau_f + v.(q_4-q_3)\;\delta_{ab}\varepsilon_{cdf}\tau_f\\ &\quad+v.(q_3-q_1)\;\delta_{bd}\varepsilon_{acf}\tau_f + v.(q_4-q_2)\;\delta_{ac}\varepsilon_{bdf}\tau_f\\ &\quad+v.(q_4-q_1)\;\delta_{bc}\varepsilon_{adf}\tau_f + v.(q_3-q_2)\;\delta_{ad}\varepsilon_{bcf}\tau_f]\end{aligned} \tag{47}$$

πN vertices from $\widehat{\mathcal{L}}^{(2)}_{\pi N}$

counterterm

$$i\left(\frac{p^2}{2m} + \frac{4M^2}{m}a_3\right) \tag{48}$$

one pion

$$\frac{\dot{g}_A}{2mF}\; v.q\; S.(p+p')\;\tau_a \tag{49}$$

two pions

$$\begin{aligned}&-\tfrac{4i}{mF^2}\;\left(a_1\; q_1.q_2 + a_2\; v.q_1\; v.q_2 + a_3 M^2\right)\;\delta_{ab}\\ &+\tfrac{1}{8mF^2}\;[(q_1-q_2)\cdot(p+p') + i16a_5\varepsilon^{\mu\nu\rho\sigma}q_{1\mu}q_{2\nu}v_\rho S_\sigma]\\ &\times\varepsilon_{abc}\tau_c\end{aligned} \tag{50}$$

πN vertices from $\widehat{\mathcal{L}}^{(3)}_{\pi N}$

one pion

$$\begin{aligned}&\tfrac{\dot{g}_A}{8m^2F}\;\left(q^2\;S\cdot q + 2\;S\cdot p'\;q\cdot p + 2\;S\cdot p\;q\cdot p'\right)\;\tau_a\\ &+\tfrac{M^2}{8\pi^2F^3}\;(b_{19}-2b_{17})\;S\cdot q\;\tau_a\end{aligned} \tag{51}$$

two pions

$$\frac{1}{8\pi^2F^4}\Big\{\big[-ib_4(v\cdot q_2\, q_1\cdot(p+p')+v\cdot q_1\, q_2\cdot(p+p'))$$
$$+(b_{16}-b_{15})\varepsilon^{\mu\nu\rho\sigma}q_{1\mu}q_{2\nu}v_\rho S_\sigma\, v\cdot(q_1-q_2)$$
$$+\frac{\overset{\circ}{g}{}_A^2\pi^2F^2}{m^2}(v\cdot q_1\, q_{2\mu}+v\cdot q_2\, q_{1\mu})\varepsilon^{\mu\nu\rho\sigma}(p-p')_\nu v_\rho S_\sigma\big]$$
$$\times\delta_{ab}+\big[-(b_1+b_2)\, q_1\cdot q_2\, v\cdot(q_1-q_2)$$
$$-b_3\, v\cdot q_1\, v\cdot q_2\, v\cdot(q_1-q_2)+2b_6M^2\, v\cdot(q_1-q_2)$$
$$+\frac{\pi^2F^2}{m^2}(8a_5+3\,\overset{\circ}{g}{}_A^2-1)\varepsilon^{\mu\nu\rho\sigma}q_{1\mu}q_{2\nu}(p+p')_\rho S_\sigma\big]$$
$$\times\varepsilon_{abc}\tau_c\Big\} \tag{52}$$

4π-vertex from $\mathcal{L}^{(2)}_{\pi\pi}$

$$\frac{i}{F^2}\,\{[(q_1+q_2)^2-M^2]\delta_{ab}\delta_{cd}$$
$$+[(q_1+q_3)^2-M^2]\delta_{ac}\delta_{bd}$$
$$+[(q_1+q_4)^2-M^2]\delta_{ad}\delta_{bc}\} \tag{53}$$

pion counterterm vertex from $\mathcal{L}^{(4)}_{\pi\pi}$

$$2i\frac{M^2}{F^2}\left[(q^2-M^2)l_4-M^2l_3\right]\delta_{ab} \tag{54}$$

B Loop integrals

Definitions

$$\Delta=-\frac{1}{i}\int\frac{d^Dk}{(2\pi)^D}\frac{1}{k^2-M^2}$$

$$I_0(Q^2)=\frac{1}{i}\int\frac{d^Dk}{(2\pi)^D}\frac{1}{(k^2-M^2)\big((k+Q)^2-M^2\big)}$$

$$Q_\mu I_1(Q^2)=\frac{1}{i}\int\frac{d^Dk}{(2\pi)^D}\frac{k_\mu}{(k^2-M^2)\big((k+Q)^2-M^2\big)}$$

$$g_{\mu\nu}I_2(Q^2)+Q_\mu Q_\nu I_3(Q^2)$$
$$=\frac{1}{i}\int\frac{d^Dk}{(2\pi)^D}\frac{k_\mu k_\nu}{(k^2-M^2)\big((k+Q)^2-M^2\big)}$$

$$J_0(\omega)=\frac{1}{i}\int\frac{d^Dk}{(2\pi)^D}\frac{1}{(k^2-M^2)(\omega-v\cdot k)}$$

$$v_\mu J_1(\omega)=\frac{1}{i}\int\frac{d^Dk}{(2\pi)^D}\frac{k_\mu}{(k^2-M^2)(\omega-v\cdot k)}$$

$$g_{\mu\nu}J_2(\omega)+v_\mu v_\nu J_3(\omega)=\frac{1}{i}\int\frac{d^Dk}{(2\pi)^D}\frac{k_\mu k_\nu}{(k^2-M^2)(\omega-v\cdot k)}$$

$$K_0(\omega,Q^2)=\frac{1}{i}\int\frac{d^Dk}{(2\pi)^D}\frac{1}{(k^2-M^2)((k+Q)^2-M^2)(\omega-v\cdot k)}$$

$$Q_\mu K_1(\omega,Q^2)+v_\mu K_1'(\omega,Q^2)$$
$$=\frac{1}{i}\int\frac{d^Dk}{(2\pi)^D}\frac{k_\mu}{(k^2-M^2)((k+Q)^2-M^2)(\omega-v\cdot k)}$$

$$g_{\mu\nu}K_2+Q_\mu Q_\nu K_3+(v_\mu Q_\nu+Q_\mu v_\nu)K_3'+v_\mu v_\nu K_3''$$
$$=\frac{1}{i}\int\frac{d^Dk}{(2\pi)^D}\frac{k_\mu k_\nu}{(k^2-M^2)((k+Q)^2-M^2)(\omega-v\cdot k)}$$

$$(Q_\lambda g_{\mu\nu}+Q_\mu g_{\nu\lambda}+Q_\nu g_{\lambda\mu})K_4$$
$$+(v_\lambda g_{\mu\nu}+v_\mu g_{\nu\lambda}+v_\nu g_{\lambda\mu})K_4'$$
$$+(v_\lambda Q_\mu Q_\nu+v_\mu Q_\nu Q_\lambda+v_\nu Q_\lambda Q_\mu)K_5 \tag{55}$$
$$+(Q_\lambda v_\mu v_\nu+Q_\mu v_\nu v_\lambda+Q_\nu v_\lambda v_\mu)K_5'$$
$$+Q_\lambda Q_\mu Q_\nu K_6+v_\lambda v_\mu v_\nu K_6'$$
$$=\frac{1}{i}\int\frac{d^Dk}{(2\pi)^D}\frac{k_\lambda k_\mu k_\nu}{(k^2-M^2)((k+Q)^2-M^2)(\omega-v\cdot k)}$$

Results[4]

$$L(\mu)=\frac{\mu^{D-4}}{16\pi^2}\left\{\frac{1}{D-4}-\frac{1}{2}\left[\ln 4\pi+1+\Gamma'(1)\right]\right\}$$
$$\Delta=2M^2\left(L(\mu)+\frac{1}{32\pi^2}\ln\frac{M^2}{\mu^2}\right) \tag{56}$$

$$I_0(Q^2)=-2L(\mu)+\frac{1}{16\pi^2}\left(1-\ln\frac{M^2}{\mu^2}-r\ln\left|\frac{1+r}{1-r}\right|\right)\quad\left[Q^2<0\right] \tag{57}$$

$$-2L(\mu)+\frac{1}{16\pi^2}\left(1-\ln\frac{M^2}{\mu^2}-2r\arctan\frac{1}{r}\right)\quad\left[0<Q^2<4M^2\right]$$

$$-2L(\mu)+\frac{1}{16\pi^2}\left(1-\ln\frac{M^2}{\mu^2}-r\ln\left|\frac{1+r}{1-r}\right|+i\pi r\right)\quad\left[Q^2>4M^2\right]$$

$$\text{where}\qquad r=\sqrt{\left|1-\frac{4M^2}{Q^2}\right|}$$

$$J_0(\omega)=-4\omega L(\mu)+\frac{\omega}{8\pi^2}\left(1-\ln\frac{M^2}{\mu^2}\right)+\frac{\sqrt{\omega^2-M^2}}{4\pi^2}\,\text{arccosh}\,\frac{-\omega}{M}\qquad[\omega<-M]$$

$$-4\omega L(\mu)+\frac{\omega}{8\pi^2}\left(1-\ln\frac{M^2}{\mu^2}\right)-\frac{\sqrt{M^2-\omega^2}}{4\pi^2}\arccos\frac{-\omega}{M}\qquad\left[\omega^2<M^2\right]$$

$$-4\omega L(\mu)+\frac{\omega}{8\pi^2}\left(1-\ln\frac{M^2}{\mu^2}\right)-\frac{\sqrt{\omega^2-M^2}}{4\pi^2}\left(\text{arccosh}\,\frac{\omega}{M}-i\pi\right)\qquad[\omega>M] \tag{58}$$

[4] Divergent integrals are calculated using dimensional regularization, with the terms in denominators of integrals understood with the $i\varepsilon$ prescription from Appendix A (i.e. $\frac{1}{k^2-M^2}$, $\frac{1}{v\cdot k-\omega}$ etc. in definitions are just abbreviations for $\frac{1}{k^2-M^2+i\varepsilon}$, $\frac{1}{v\cdot k-\omega+i\varepsilon}$ etc). Results are given in the limit $D\to 4$, i.e. in the final formulae the dimension of space-time $D=4-2\varepsilon$ is expanded in powers of ε, then one uses $\varepsilon L=-\frac{1}{32\pi^2}+\mathcal{O}(\varepsilon)$ and afterwards ε is sent to zero

$$K_0(0,Q^2) = -\frac{1}{8\pi\sqrt{-Q^2}} \arctan\frac{\sqrt{-Q^2}}{2M} \quad \left[v\cdot Q = 0 \quad \text{and} \quad Q^2 < 0\right]$$
$$\frac{1}{16\pi\sqrt{Q^2}} \ln\frac{2M-\sqrt{Q^2}}{2M+\sqrt{Q^2}} \quad \left[v\cdot Q = 0 \quad \text{and} \quad 0 < Q^2 < 4M^2\right]$$
$$\frac{1}{16\pi\sqrt{Q^2}} \left(\ln\frac{\sqrt{Q^2}-2M}{\sqrt{Q^2}+2M} + i\pi\right) \quad \left[v\cdot Q = 0 \quad \text{and} \quad Q^2 > 4M^2\right] \tag{59}$$

$$I_1(Q^2) = -\tfrac{1}{2} I_0(Q^2)$$
$$I_2(Q^2) = \tfrac{1}{3}\left(\left(M^2 - \tfrac{Q^2}{4}\right) I_0(Q^2) - \tfrac{1}{2}\Delta + \tfrac{1}{16\pi^2}\left(M^2 - \tfrac{Q^2}{6}\right)\right) \tag{60}$$
$$I_3(Q^2) = \tfrac{1}{3}\left(\left(1 - \tfrac{M^2}{Q^2}\right) I_0(Q^2) - \tfrac{1}{2Q^2}\Delta - \tfrac{1}{16\pi^2}\left(\tfrac{M^2}{Q^2} - \tfrac{1}{6}\right)\right)$$

$$J_1(\omega) = \omega J_0(\omega) + \Delta$$
$$J_2(\omega) = \tfrac{1}{3}\left(\left(M^2 - \omega^2\right) J_0(\omega) - \omega\Delta + \tfrac{1}{8\pi^2}\left(\omega M^2 - \tfrac{2}{3}\omega^3\right)\right) \tag{61}$$
$$J_3(\omega) = \omega J_1(\omega) - J_2(\omega)$$

$$K_1(0,Q^2) = -\tfrac{1}{2} K_0(0,Q^2)$$
$$K_1'(0,Q^2) = -I_0(Q^2)$$
$$K_2(0,Q^2) = \tfrac{1}{2}\left(M^2 - \tfrac{1}{4}Q^2\right) K_0(0,Q^2) + \tfrac{1}{4} J_0(0)$$
$$K_3(0,Q^2) = \left(\tfrac{3}{8} - \tfrac{M^2}{2Q^2}\right) K_0(0,Q^2) + \tfrac{1}{4Q^2} J_0(0)$$
$$K_3'(0,Q^2) = -I_1(Q^2)$$
$$K_3''(0,Q^2) = -K_2(0,Q^2)$$
$$K_4(0,Q^2) = -\tfrac{1}{4} J_0(0) + \tfrac{1}{2} M^2 K_1(0,Q^2) + \tfrac{1}{4} K_2(0,Q^2) + \tfrac{1}{4} Q^2 K_3(0,Q^2)$$
$$K_4'(0,Q^2) = \tfrac{1}{3}\left(\tfrac{Q^2}{4} - M^2\right) I_0(Q^2) + \tfrac{1}{6}\Delta + \tfrac{1}{48\pi^2}\left(\tfrac{Q^2}{6} - M^2\right)$$
$$K_5(0,Q^2) = -\tfrac{1}{4} I_0(Q^2) + \tfrac{1}{2Q^2}\Delta - \tfrac{1}{Q^2} K_4'(0,Q^2)$$
$$K_5'(0,Q^2) = -K_4(0,Q^2)$$
$$K_6(0,Q^2) = -\tfrac{1}{Q^2} J_0(0) + \tfrac{M^2}{Q^2} K_1(0,Q^2) - \tfrac{5}{Q^2} K_4(0,Q^2)$$
$$K_6'(0,Q^2) = -I_2(Q^2) - 3K_4'(0,Q^2) \tag{62}$$

where all the $\mathbf{K}_i(\mathbf{0},\mathbf{Q}^2)$ are given only **for** $\mathbf{v}\cdot\mathbf{Q} = \mathbf{0}$

C Feynman diagrams for πN scattering

Amplitudes corresponding to Feynman diagrams in Fig. 1–4 are presented. On-shell conditions

$$q^2 = q'^2 = M_\pi^2 \qquad v\cdot q - v\cdot q' = \mathcal{O}(p^2) \tag{63}$$

are used to simplify expressions. Amplitudes are given in terms of loop integrals defined in Appendix B and the following notation is used

$$J_n^{\pm}(w) = J_n(w) \pm J_n(-w) \quad . \tag{64}$$

first order

Fig. 1a

$$\alpha^+ = \tfrac{\dot{g}_A^2}{4F^2}\left(\tfrac{1}{w} - \tfrac{1}{w'}\right)(q\cdot q' - ww') \qquad \beta^+ = \tfrac{\dot{g}_A^2}{2F^2}\left(\tfrac{1}{w} + \tfrac{1}{w'}\right)$$
$$\alpha^- = \tfrac{\dot{g}_A^2}{4F^2}\left(\tfrac{1}{w} + \tfrac{1}{w'}\right)(q\cdot q' - ww') \qquad \beta^- = \tfrac{\dot{g}_A^2}{2F^2}\left(\tfrac{1}{w} - \tfrac{1}{w'}\right) \tag{65}$$

Fig. 1b

$$\alpha^+ = 0 \qquad \beta^+ = 0 \qquad \alpha^- = \tfrac{1}{4F^2}(w + w') \qquad \beta^- = 0 \tag{66}$$

second order

Fig. 2a

$$\alpha^+ = -\tfrac{\dot{g}_A^2}{4mF^2}(q\cdot q' - ww') \qquad \beta^+ = 0 \qquad \alpha^- = 0 \qquad \beta^- = -\tfrac{\dot{g}_A^2}{2mF^2} \tag{67}$$

Fig. 2b

$$\alpha^+ = \tfrac{\dot{g}_A^2}{8mF^2}\left[4ww' - w^2 - w'^2 + (q\cdot q' - 2M_\pi^2)\left(\tfrac{w'}{w} + \tfrac{w}{w'}\right)\right]$$
$$\beta^+ = \tfrac{\dot{g}_A^2}{4mF^2}\left(\tfrac{w'}{w} - \tfrac{w}{w'}\right)$$
$$\alpha^- = \tfrac{\dot{g}_A^2}{8mF^2}\left[w^2 - w'^2 + (q\cdot q' - 2M_\pi^2)\left(\tfrac{w'}{w} - \tfrac{w}{w'}\right)\right]$$
$$\beta^- = \tfrac{\dot{g}_A^2}{4mF^2}\left(\tfrac{w'}{w} + \tfrac{w}{w'}\right) \tag{68}$$

Fig. 2c

$$\alpha^+ = -\frac{\dot{g}_A^2 M^2}{8mF^2}\left(\frac{1}{w^2}+\frac{1}{w'^2}\right)(q\cdot q' - ww') \tag{69}$$
$$\beta^+ = -\frac{\dot{g}_A^2 M^2}{4mF^2}\left(\frac{1}{w^2}-\frac{1}{w'^2}\right)$$
$$\alpha^- = -\frac{\dot{g}_A^2 M^2}{8mF^2}\left(\frac{1}{w^2}-\frac{1}{w'^2}\right)(q\cdot q' - ww')$$
$$\beta^- = -\frac{\dot{g}_A^2 M^2}{4mF^2}\left(\frac{1}{w^2}+\frac{1}{w'^2}\right)$$

Fig. 2d

$$\alpha^+ = \frac{4}{mF^2}\left(a_1 q.q' + a_2 ww' - a_3 M^2\right) \tag{70}$$
$$\beta^+ = 0$$
$$\alpha^- = 0$$
$$\beta^- = -\frac{2}{mF^2}a_5$$

third order

Fig. 3a+3b

$$\alpha^+ = 0 \tag{71}$$
$$\beta^+ = \frac{\dot{g}_A^2}{4m^2F^2}\frac{1}{w}\left[\frac{M^2m^2}{\pi^2F^2\dot{g}_A}(2b_{17}-b_{19}) - M_\pi^2 + q\cdot q'\right]$$
$$\alpha^- = \frac{\dot{g}_A^2}{8m^2F^2}\frac{1}{w}\Bigg\{\left[\frac{M^2m^2}{\pi^2F^2\dot{g}_A}(2b_{17}-b_{19}) - M_\pi^2\right] \times \left(q\cdot q' - w^2\right) + \left(q\cdot q' - M_\pi^2 + w^2\right)\left(q\cdot q' - M_\pi^2\right)\Bigg\}$$
$$\beta^- = 0$$

Fig. 3c

$$\alpha^+ = 0 \tag{72}$$
$$\beta^+ = -\frac{\dot{g}_A^2}{4m^2F^2}w$$
$$\alpha^- = -\frac{\dot{g}_A^2}{8m^2F^2}w\left(q\cdot q' + w^2 - 2M_\pi^2\right)$$
$$\beta^- = 0$$

Fig. 3d

$$\alpha^+ = 0 \tag{73}$$
$$\beta^+ = \frac{1}{4\pi^2F^4}w\left[b_{16} - b_{15} + \frac{\dot{g}_A^2\pi^2F^2}{m^2}\right]$$
$$\alpha^- = \frac{1}{4\pi^2F^4}w\left[(b_1+b_2)\,q\cdot q' + b_3w^2 + 2b_6M^2\right]$$
$$\beta^- = 0$$

Fig. 3e+3f

$$\alpha^+ = 0 \tag{74}$$
$$\beta^+ = 0$$
$$\alpha^- = \frac{\dot{g}_A^2M^2}{4m^2F^2}\frac{1}{w}\left(M^2 - w^2\right)$$
$$\beta^- = 0$$

Fig. 3g

$$\alpha^+ = \frac{3g_A^4M^3}{64\pi F^4}\frac{1}{w^2}\left(q\cdot q' - w^2\right) \tag{75}$$
$$\beta^+ = \frac{\dot{g}_A^2M^2}{4m^2F^2}\frac{1}{w}\left(\frac{M^2}{w^2} + 16a_3\right)$$
$$\alpha^- = \frac{\dot{g}_A^2M^2}{8m^2F^2}\frac{1}{w}\left(\frac{M^2}{w^2} + 16a_3\right)\left(q\cdot q' - w^2\right)$$
$$\beta^- = \frac{3g_A^4M^3}{32\pi F^4}\frac{1}{w^2}$$

Fig. 4a, 4b

$$0$$

Fig. 4c+4d

$$\alpha^+ = -\frac{\dot{g}_A^4}{8F^4}\frac{1}{w^2}\left(J_2^+(w) - 2J_2(0)\right)\left(q\cdot q' - w^2\right) \tag{76}$$
$$\beta^+ = -\frac{\dot{g}_A^4}{4F^4}\frac{1}{w^2}\left(J_2^-(w) + \frac{1}{6\pi^2}w^3 - \frac{1}{4\pi^2}M^2w\right)$$
$$\alpha^- = -\frac{\dot{g}_A^4}{8F^4}\frac{1}{w^2}\left(J_2^-(w) + \frac{1}{6\pi^2}w^3 - \frac{1}{4\pi^2}M^2w\right) \times \left(q\cdot q' - w^2\right)$$
$$\beta^- = -\frac{\dot{g}_A^4}{4F^4}\frac{1}{w^2}\left(J_2^+(w) - 2J_2(0)\right)$$

Fig. 4e

$$\alpha^+ = \frac{3\dot{g}_A^4}{16F^4}\frac{1}{w^2}\left(M^2 - w^2\right)J_0^+(w)\left(q\cdot q' - w^2\right) \tag{77}$$
$$\beta^+ = \frac{3\dot{g}_A^4}{8F^4}\frac{1}{w^2}\left(\left(M^2 - w^2\right)J_0^-(w) - 2w\Delta\right)$$
$$\alpha^- = \frac{3\dot{g}_A^4}{16F^4}\frac{1}{w^2}\left(\left(M^2 - w^2\right)J_0^-(w) - 2w\Delta\right) \times \left(q\cdot q' - w^2\right)$$
$$\beta^- = \frac{3\dot{g}_A^4}{8F^4}\frac{1}{w^2}\left(M^2 - w^2\right)J_0^+(w)$$

Fig. 4f

$$\alpha^+ = \frac{1}{8F^4}\left(w^2J_0^+(w) + 3wJ_1^-(w)\right) \tag{78}$$
$$\beta^+ = 0$$
$$\alpha^- = \frac{1}{16F^4}\left(w^2J_0^-(w) + 3wJ_1^+(w)\right)$$
$$\beta^- = 0$$

Fig. 4g, 4h

$$0$$

Fig. 4i

$$\alpha^+ = \frac{9\dot{g}_A^4}{16F^4}\frac{1}{w^2}\left(J_2^+(w) - 2J_2(0)\right)\left(q\cdot q' - w^2\right) \tag{79}$$
$$\beta^+ = \frac{3\dot{g}_A^4}{8F^4}\frac{1}{w^2}\left(-J_2^-(w) + 2w\frac{\partial J_2(0)}{\partial\omega} + \frac{1}{6\pi^2}w^3\right)$$
$$\alpha^- = \frac{3\dot{g}_A^4}{16F^4}\frac{1}{w^2}\left(-J_2^-(w) + 2w\frac{\partial J_2(0)}{\partial\omega} - \frac{1}{18\pi^2}w^3\right) \times \left(q\cdot q' - w^2\right)$$
$$\beta^- = \frac{\dot{g}_A^4}{8F^4}\frac{1}{w^2}\left(J_2^+(w) - 2J_2(0)\right)$$

Fig. 4k

$$\alpha^+ = 0 \tag{80}$$
$$\beta^+ = 0$$
$$\alpha^- = -\tfrac{1}{F^4} w I_2(t)$$
$$\beta^- = 0$$

Fig. 4l

$$\alpha^+ = \tfrac{\dot{g}_A^2}{4F^4}\left[(3t - M^2)tK_1(0,t) \right. \tag{81}$$
$$+ \ (11t - 3M^2)K_2(0,t)$$
$$+ \ (5t - M^2)tK_3(0,t) + 10tK_4(0,t)$$
$$\left. + \ 2t^2 K_6(0,t) + 6J_2(0)\right]$$
$$\beta^+ = 0$$
$$\alpha^- = \tfrac{\dot{g}_A^2}{F^4} w \left[tK_3'(0,t) + tK_5(0,t) + (\tfrac{t}{4} - M^2)I_0(t) + \tfrac{1}{2}\Delta\right]$$
$$\beta^- = -\tfrac{\dot{g}_A^2}{F^4}\ 2K_2(0,t)$$

Fig. 4m

$$\alpha^+ = 0 \tag{82}$$
$$\beta^+ = 0$$
$$\alpha^- = \tfrac{\dot{g}_A^2}{8F^4} w \left(3\tfrac{\partial J_2(0)}{\partial \omega} - \tfrac{M^2}{8\pi^2}\right)$$
$$\beta^- = 0$$

Fig. 4n, 4o

$$0$$

Fig. 4p+4r

$$\alpha^+ = 0 \tag{83}$$
$$\beta^+ = \tfrac{\dot{g}_A^2}{F^4}\tfrac{1}{w}\Delta$$
$$\alpha^- = \tfrac{\dot{g}_A^2}{2F^4}\tfrac{1}{w}\Delta\left(q \cdot q' - w^2\right)$$
$$\beta^- = 0$$

Fig. 4s

$$0$$

Fig. 4t+4u

$$\alpha^+ = -\tfrac{3g_A^2}{2F^4} J_2(0) \tag{84}$$
$$\beta^+ = 0$$
$$\alpha^- = 0$$
$$\beta^- = 0$$

Fig. 4v

$$\alpha^+ = 0 \tag{85}$$
$$\beta^+ = 0$$
$$\alpha^- = \tfrac{5}{8F^4} w \Delta$$
$$\beta^- = 0$$

external legs (wave function) renormalization

$$\alpha^+ = 0 \tag{86}$$
$$\beta^+ = \tfrac{\dot{g}_A^2}{F^2}\tfrac{1}{w}\left(\tfrac{1}{2}\delta Z_N(p) + \tfrac{1}{2}\delta Z_N(p') + \delta Z_\pi\right)$$
$$\alpha^- = \left[\tfrac{\dot{g}_A^2}{2F^2}\tfrac{1}{w}\left(q \cdot q' - w^2\right) + \tfrac{1}{2F^2} w\right]$$
$$\times \left(\tfrac{1}{2}\delta Z_N(p) + \tfrac{1}{2}\delta Z_N(p') + \delta Z_\pi\right)$$
$$\beta^- = 0$$

$$\delta Z_N(p) = \tfrac{4M_\pi^2 a_3}{m_N^2} - \tfrac{3g_A^2 M_\pi^2}{32\pi^2 F_\pi^2}\left[1 + 48\pi^2 L(\mu) + 3\ln\tfrac{M_\pi}{\mu}\right]$$
$$\delta Z_N(p') = \tfrac{4M_\pi^2 a_3}{m_N^2} + \tfrac{t}{4m_N^2}$$
$$- \tfrac{3g_A^2 M_\pi^2}{32\pi^2 F_\pi^2}\left[1 + 48\pi^2 L(\mu) + 3\ln\tfrac{M_\pi}{\mu}\right]$$
$$\delta Z_\pi = -\tfrac{M_\pi^2}{8\pi^2 F_\pi^2}\left[\bar{l}_4 + 48\pi^2 L(\mu) + \ln\tfrac{M_\pi}{\mu}\right]$$

D Scattering lengths, volumes, ...

Threshold parameters for the first four partial waves are given in explicit form, order by order. In the third order, the general formulae are displayed only if they are reasonably short, otherwise only the numerical results are given (in appropriate powers of GeV).

S-wave

1st order

$$a_0^+ = 0$$

$$b_0^+ = 0$$

$$a_0^- = \tfrac{m_N M_\pi}{8\pi F_\pi^2 (m_N + M_\pi)} \tag{87}$$

$$b_0^- = \tfrac{2m_N^2 + 3M_\pi^2 - 4g_A^2 M_\pi (m_N + M_\pi)}{32\pi F_\pi^2 M_\pi m_N (m_N + M_\pi)}$$

2nd order

$$a_0^+ = \frac{(a_1+a_2-a_3)M_\pi^2}{\pi F_\pi^2(m_N+M_\pi)}$$

$$b_0^+ = \frac{a_1\left(4m_N^2-2m_N M_\pi+M_\pi^2\right)+a_2\left(4m_N^2+2m_N M_\pi+5M_\pi^2\right)+a_3\left(2m_N M_\pi-M_\pi^2\right)}{4\pi F_\pi^2 m_N^2(m_N+M_\pi)} + \frac{g_A^2\left(2m_N^2+3m_N M_\pi+3M_\pi^2\right)}{16\pi F_\pi^2 m_N^2(m_N+M_\pi)}$$

$$a_0^- = 0$$

$$b_0^- = \frac{g_A^2 M_\pi}{8\pi F_\pi^2 m_N(m_N+M_\pi)} \tag{88}$$

3rd order

$$a_0^+ = \frac{3g_A^2 m_N M_\pi^3}{256\pi^2 F_\pi^4(m_N+M_\pi)}$$

$$b_0^+ = \frac{g_A^2 M_\pi\left(154m_N^2-18m_N M_\pi+9M_\pi^2\right)-g_A^4 M_\pi^2(128m_N+64M_\pi)}{3072\pi^2 F_\pi^4 m_N(m_N+M_\pi)}$$

$$a_0^- = \frac{M_\pi^3 a_3}{2\pi F_\pi^2 m_N(m_N+M_\pi)} + \frac{m_N^2 M_\pi^3\left[\frac{1}{4}+\widetilde{b}_1+\widetilde{b}_2+\widetilde{b}_3+2\widetilde{b}_6\right]}{16\pi^3 F_\pi^4 m_N(m_N+M_\pi)}$$

$$b_0^- = -0.16+1.48a_3+5.15\left(\widetilde{b}_1+\widetilde{b}_2\right)+6.18\widetilde{b}_3 + 3.82\widetilde{b}_6+0.64b_{19} \tag{89}$$

P-wave

1st order

$$a_{1+}^+ = \frac{g_A^2}{24\pi F_\pi^2 M_\pi}$$

$$a_{1-}^+ = -\frac{g_A^2}{12\pi F_\pi^2 M_\pi}$$

$$a_{1+}^- = \frac{M_\pi-2g_A^2(m_N+M_\pi)}{48\pi F_\pi^2 M_\pi(m_N+M_\pi)}$$

$$a_{1-}^- = \frac{2m_N M_\pi-3M_\pi^2-4g_A^2 m_N(m_N+M_\pi)}{96\pi F_\pi^2 M_\pi m_N(m_N+M_\pi)} \tag{90}$$

2nd order

$$a_{1+}^+ = \frac{-16m_N a_1+16M_\pi a_2+g_A^2(m_N+3M_\pi)}{48\pi F_\pi^2 m_N(m_N+M_\pi)}$$

$$a_{1-}^+ = \frac{-a_1\left(16m_N^2+12M_\pi^2\right)+a_2\left(16m_N M_\pi-12M_\pi^2\right)+12a_3 M_\pi^2+g_A^2 m_N(m_N+3M_\pi)}{48\pi F_\pi^2 m_N^2(m_N+M_\pi)}$$

$$a_{1+}^- = -\frac{4a_5(m_N+M_\pi)+g_A^2(m_N+3M_\pi)}{48\pi F_\pi^2 m_N(m_N+M_\pi)}$$

$$a_{1-}^- = \frac{4a_5(m_N+M_\pi)+g_A^2 m_N}{24\pi F_\pi^2 m_N(m_N+M_\pi)} \tag{91}$$

3rd order

$$a_{1+}^+ = -6.47+0.62\left(b_{16}-\widetilde{b}_{15}\right)-0.78b_{19}$$

$$a_{1-}^+ = -8.60-1.24\left(b_{16}-\widetilde{b}_{15}\right)+1.56b_{19}$$

$$a_{1+}^- = 2.61-1.08\left(\widetilde{b}_1+\widetilde{b}_2\right)+0.68b_{19} \tag{92}$$

$$a_{1-}^- = -6.94-0.014a_3-1.10\left(\widetilde{b}_1+\widetilde{b}_2\right) - 0.018\widetilde{b}_3-0.035\widetilde{b}_6+0.68b_{19}$$

D-wave

1st order

$$a_{2+}^+ = -\frac{g_A^2}{60\pi F_\pi^2 M_\pi^2 m_N}$$

$$a_{2-}^+ = \frac{g_A^2(2m_N+5M_\pi)}{480\pi F_\pi^2 M_\pi^2 m_N^2}$$

$$a_{2+}^- = \frac{g_A^2}{60\pi F_\pi^2 M_\pi^2 m_N} \tag{93}$$

$$a_{2-}^- = -\frac{g_A^2\left(4m_N^2-6m_N M_\pi-10M_\pi^2\right)+5M_\pi^2}{960\pi F_\pi^2 M_\pi^2 m_N^2(m_N+M_\pi)}$$

2nd order

$$a_{2+}^{+}=-\frac{g_A^2(m_N+2M_\pi)}{120\pi F_\pi^2 M_\pi m_N^2(m_N+M_\pi)}$$

$$a_{2-}^{+}=\frac{80a_1 m_N M_\pi-80a_2 M_\pi^2-g_A^2\left(8m_N^2+21m_N M_\pi+15M_\pi^2\right)}{960\pi F_\pi^2 M_\pi m_N^3(m_N+M_\pi)}$$

$$a_{2+}^{-}=\frac{g_A^2(m_N+2M_\pi)}{120\pi F_\pi^2 M_\pi m_N^2(m_N+M_\pi)} \tag{94}$$

$$a_{2-}^{-}=-\frac{20a_5 M_\pi(m_N+M_\pi)+g_A^2\left(12\,m_N^2+9m_N M_\pi-5M_\pi^2\right)}{960\pi F_\pi^2 M_\pi m_N^3(m_N+M_\pi)}$$

3rd order

$$a_{2+}^{+}=\frac{193g_A^2 m_N}{115200\pi^2 F_\pi^4 M_\pi(m_N+M_\pi)}$$

$$a_{2-}^{+}=25.0+0.18\left(b_{16}-\widetilde{b}_{15}\right)-0.22b_{19}$$

$$a_{2+}^{-}=\frac{\left[1+g_A^2(7-5\pi)\right]m_N-5\pi g_A^2 M_\pi}{14400\pi^3 F_\pi^4 M_\pi(m_N+M_\pi)} \tag{95}$$

$$a_{2-}^{-}=11.5+0.306\left(\widetilde{b}_1+\widetilde{b}_2\right)-0.193b_{19}$$

F-wave

1st order

$$a_{3+}^{+}=\frac{g_A^2}{140\pi F_\pi^2 M_\pi^3 m_N^2}$$

$$a_{3-}^{+}=-\frac{g_A^2}{840\pi F_\pi^2 M_\pi^3 m_N^2}$$

$$a_{3+}^{-}=-\frac{g_A^2}{140\pi F_\pi^2 M_\pi^3 m_N^2} \tag{96}$$

$$a_{3-}^{-}=\frac{g_A^2}{840\pi F_\pi^2 M_\pi^3 m_N^2}$$

2nd order

$$a_{3+}^{+}=\frac{g_A^2(2m_N+3M_\pi)}{280\pi F_\pi^2 M_\pi^2 m_N^3(m_N+M_\pi)}$$

$$a_{3-}^{+}=-\frac{g_A^2\left(4m_N^2-15m_N M_\pi-14M_\pi^2\right)}{3360\pi F_\pi^2 M_\pi^2 m_N^4(m_N+M_\pi)}$$

$$a_{3+}^{-}=-\frac{g_A^2(2m_N+3M_\pi)}{280\pi F_\pi^2 M_\pi^2 m_N^3(m_N+M_\pi)} \tag{97}$$

$$a_{3-}^{-}=\frac{g_A^2(4m_N-M_\pi)}{3360\pi F_\pi^2 M_\pi^2 m_N^3(m_N+M_\pi)}$$

3rd order

$$a_{3+}^{+}=\frac{73g_A^2 m_N}{752640\pi^2 F_\pi^4 M_\pi^3(m_N+M_\pi)}$$

$$a_{3-}^{+}=\frac{g_A^2\left(2190m_N^2-9457M_\pi^2\right)}{22579200\pi^2 F_\pi^4 M_\pi^3 m_N(m_N+M_\pi)}$$

$$a_{3+}^{-}=\frac{m_N\left[2+g_A^2(18-7\pi)\right]-7\pi g_A^2 M_\pi}{470400\pi^3 F_\pi^4 M_\pi^3(m_N+M_\pi)} \tag{98}$$

$$a_{3-}^{-}=23.3$$

Acknowledgements. I owe much to G. Ecker, this work would be impossible without his continuous help. I would also like to thank H. Leutwyler for useful comments to the first version of the manuscript and R. Lietava and V. Černý for helpful discussions. And last but not least, a very useful correspondence with N. Kaiser and U.-G. Meißner in the final stage of the work is acknowledged with pleasure.

References

1. S. Weinberg, Phys. Rev. Lett. 17 (1966) 616
2. J. Gasser and H. Leutwyler, Ann. Phys. (N.Y.) 158 (1984) 142; Nucl. Phys. B250 (1985) 465
3. J. Gasser, M.E. Sainio and A. Švarc, Nucl. Phys. B307 (1988) 779
4. S. Weinberg, Physica 96A(1979) 327
5. E. Jenkins and A.V. Manohar, Phys. Lett. B255 (1991) 558
6. V. Bernard, N. Kaiser and U.-G. Meißner, Int. J. Mod. Phys. E4 (1995) 193
7. V. Bernard, N. Kaiser and U.-G. Meißner, Phys. Rev. C52 (1995) 2185
8. B. Borasoy and U.-G. Meißner, Ann. Phys.(NY) 254 (1997) 192
9. V. Bernard, N. Kaiser and U.-G. Meißner, Phys. Lett. B309 (1993) 421
10. V. Bernard, N. Kaiser and U.-G. Meißner, Nucl. Phys. A615 (1997) 483
11. G. Ecker, J. Gasser, A. Pich and E. de Rafael, Nucl. Phys. B321 (1989) 311
12. T. Mannel, W. Roberts and Z. Ryzak, Nucl. Phys. B368 (1992) 315
13. G. Ecker and M. Mojžiš, Phys. Lett. B365 (1996) 312
14. V. Bernard, N. Kaiser, J. Kambor and U.-G. Meißner, Nucl. Phys. B388 (1992) 315
15. H. Fearing, R. Lewis, N. Mobed and S. Scherer, Muon capture by a proton in heavy baryon chiral perturbation theory, hep-ph/9702394
16. G. Ecker and M. Mojžiš, Wave function renormalization in heavy baryon chiral perturbation theory, hep-ph/9705216
17. G. Ecker, Phys. Lett. B336 (1994) 508
18. G. Höhler, in Landolt-Börnstein, vol. 9 b2, ed. H. Schopper (Springer, Berlin, 1983)
19. G. Höhler and H.M.Staudenmaier, πN Newsletter 11 (1996)
20. R. Koch and E. Pietarinen, Nucl. Phys. A336 (1980) 331